Free Radical Biology and Medicine 124 (2018) 319–327

Contents lists available at ScienceDirect

Free Radical Biology and Medicine

journal homepage: www.elsevier.com/locate/freeradbiomed

Original article

C_{60} fullerene accumulation in human leukemic cells and perspectives of LED-mediated photodynamic therapy

Anna Grebinyk[a,b,c], Sergii Grebinyk[a], Svitlana Prylutska[d], Uwe Ritter[e], Olga Matyshevska[c], Thomas Dandekar[b], Marcus Frohme[a,*]

[a] Division Molecular Biotechnology and Functional Genomics, Technical University of Applied Sciences Wildau, Hochschulring 1, 15745 Wildau, Germany
[b] Dept. of Bioinformatics, Biocenter, University of Würzburg, Am Hubland, 97074 Würzburg, Germany
[c] Educational and Scientific Center "Institute of Biology and Medicine", Taras Shevchenko National University of Kyiv, Volodymyrska 64, 01601 Kyiv, Ukraine
[d] Dept. of Chemistry, Taras Shevchenko National University of Kyiv, Volodymyrska 64, 01601 Kyiv, Ukraine
[e] Institute of Chemistry and Biotechnology, University of Technology Ilmenau, Weimarer Straße 25 (Curiebau), 98693 Ilmenau, Germany

ARTICLE INFO

Keywords:
C_{60} fullerene
Photodanamic therapy
LEDs
Leukemic cells
Immunocytochemistry
HPLC-ESI-MS
Apoptosis

ABSTRACT

Recent progress in nanobiotechnology has attracted interest to a biomedical application of the carbon nanostructure C_{60} fullerene since it possesses a unique structure and versatile biological activity. C_{60} fullerene potential application in the frame of cancer photodynamic therapy (PDT) relies on rapid development of new light sources as well as on better understanding of the fullerene interaction with cells.

The aim of this study was to analyze C_{60} fullerene effects on human leukemic cells (CCRF-CEM) in combination with high power single chip light-emitting diodes (LEDs) light irradiation of different wavelengths: ultraviolet (UV, 365 nm), violet (405 nm), green (515 nm) and red (632 nm). The time-dependent accumulation of fullerene C_{60} in CCRF-CEM cells up to 250 ng/10^6 cells at 24 h with predominant localization within mitochondria was demonstrated with immunocytochemical staining and liquid chromatography mass spectrometry. In a cell viability assay we studied photoexcitation of the accumulated C_{60} nanostructures with ultraviolet or violet LEDs and could prove that significant phototoxic effects did arise. A less pronounced C_{60} fullerene phototoxic effect was observed after irradiation with green, and no effect was detected with red light. A C_{60} fullerene photoactivation with violet light induced substantial ROS generation and apoptotic cell death, confirmed by caspase3/7 activation and plasma membrane phosphatidylserine externalization. Our work proved C_{60} fullerene ability to induce apoptosis of leukemic cells after photoexcitation with high power single chip 405 nm LED as a light source. This underlined the potential for application of C_{60} nanostructure as a photosensitizer for anticancer therapy.

1. Introduction

Photodynamic therapy is a non-surgical approach aimed on the selective elimination of cancer cells. The main idea of PDT is to combine two non-toxic components – photosensitizing molecule and visible light – which in the presence of oxygen gain a pronounced toxicity [1–3]. Anticancer PDT effects are realized directly through the induction of cancer cell death and/or indirectly when damage of the vascular system and activation of the immune response are provoked [4,5]. Rapid development of endoscopic fiber optic devices [6,7] allows to test PDT in treatment not only for skin malignacies, but for brain, lung, esophagus, colon, pancreas, liver, bile duct, breast, bladder, prostate and neck cancers as well [1,4,8].

Over the past decade, the application of nanoparticulate agents has been established both in pharmaceutical research and in clinical settings [4,9]. The constantly increasing interest in novel nanotechnology platforms for biomedical applications stimulated the investigation of carbon nanomaterials, including fullerenes and their most prominent representative – C_{60} fullerene [10]. Pristine non-modified C_{60} fullerene is a lipophilic, spheroidal shaped and symmetrical molecule with 0.72 nm in diameter [11,12]. Due to the specific packing of atoms in penta- and hexagon units the surface of C_{60} is three times smaller than expected for biological molecules with the same molecular weight of 720 Da. The unusual structure of C_{60} fullerene determines its unique physicochemical properties and biological activity [9,11–14].

Today considerable attention is devoted to C_{60} fullerene as potential

Abbreviation: HPLC-ESI-MS, High Performance Liquid Chromatography-Electro Spray Ionization -Mass Spectrometry

* Corresponding author.
E-mail address: mfrohme@th-wildau.de (M. Frohme).

https://doi.org/10.1016/j.freeradbiomed.2018.06.022
Received 22 March 2018; Received in revised form 29 May 2018; Accepted 20 June 2018
Available online 27 June 2018
0891-5849/ © 2018 The Author(s). Published by Elsevier Inc. This is an open access article under the CC BY license (http://creativecommons.org/licenses/BY/4.0/).

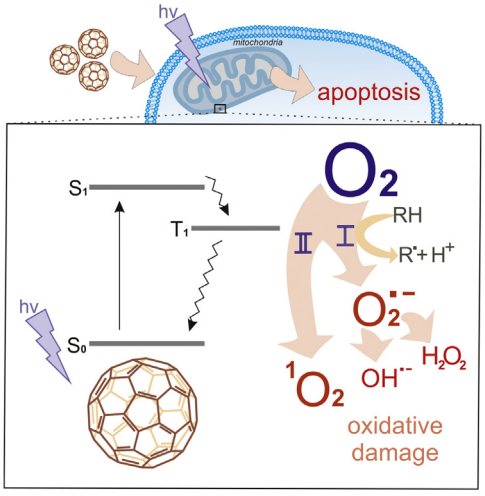

Fig. 1. Schematic mechanism of C_{60} fullerene photodynamic cancer therapy. An absorbed photon excites C_{60} fullerene to the first excited singlet state S_1, that relaxes to the more long lived triplet state T_1. The C_{60} triplet interacts with oxygen either through type I or type II, resulting in the intensification of reactive oxygen species generation and induction of apoptotic cell death.

regulator of oxidative balance in biological systems. Since a C_{60} molecule consists entirely of sp^2-hybridized carbon atoms [14], it is able to generate reactive oxygen species (ROS) after UV–vis light irradiation with a quantum yield of 1.0 [15]. C_{60} fullerene advantages compared to conventional photosensitizing molecules are the higher photostability and lesser photobleaching [2]. There are two ways of ROS production by photoexcited C_{60}: by energy (type I) or electron (type II) transfer from photoexcited C_{60} to oxygen (Fig. 1) [2,15–19]. The produced reactive oxygen species are excellent oxidizing agents that react with a wide range of biological targets. Oxidative stress, which occurs when ROS generation overwhelms the cell antioxidant defense system can lead to cell death by apoptosis [16–18]. Mitochondria have been found to be an important subcellular target for many photosensitizing drugs due to its role in apoptosis induction [3,17].

C_{60} fullerene-mediated PDT efficiency in vitro and in vivo was shown to a large extent with its hydrophilic derivatives hydroxy- [14,17,20], carboxy- [16], PEG [10,12,17] -C_{60} and C_{60} with various organic substitutes [15,18,20–23]. Functionalization of C_{60} improves its water solubility and increases its biocompatibility by decreasing the aggregate size [14], but on the other hand, inhibits its interaction with cellular lipid membranes and changes the pattern of cellular uptake [14,18,19,22,23]. C_{60} diffuses through bilayered membrane from six [22] to nine [24] orders of magnitude faster as compared with its hydrophilic derivatives, which interact with polar groups on the membrane surface instead of entering the cell. Higher lipophilicity promotes diffusion of pharmaceutical agents across the plasma membrane and further relocation to other cellular membranes, thus facilitating intracellular uptake [17]. Hydrophobic drugs are shown to attack the cancer cells mainly by direct interactions, weather hydrophilic agents act indirectly by damaging blood vessels [18]. Moreover, the presence of functional groups on C_{60} fullerene surface decreases the quantum yield of singlet oxygen production after molecule photoexcitation [15,16]. So, the cellular uptake and further biological effects of pristine C_{60} and its derivatives could be different. Pristine C_{60} fullerene may be applied in PTD in the form of liposome-based delivery systems [2,8,16,25,26] or water colloidal C_{60} solutions [16,27–30]. Previously, a negligible toxicity of pristine C_{60} stable colloid solution [30] against normal cells was shown [29,30]. At the same time a pronounced proapoptotic effect was detected in leukemic cells treated with pristine C_{60} fullerene and irradiated with UV/Vis light in the range of 320–600 nm [11,27,31]. These data indicate the potential of C_{60} as an effective photosensitizer in cancer therapy.

The use of high power single chip light-emitting diodes is expected to promote PDT application, since they have a higher portability and extremely lower cost, compromising the efficiency [32,33] of lasers as the classical PDT light sources. LED-based equipment has a high potential to simplify PDT's technical part and to reduce costs [34]. In this paper, we report first data concerning the pristine C_{60} fullerene accumulation and localization inside human leukemic cells and its phototoxic effects potentially induced by UV, violet, green and red high power single chip LEDs light irradiation.

2. Materials and methods

2.1. Chemicals

RPMI 1640 liquid medium, phosphate buffered saline (PBS), Fetal Bovine Serum (FBS), Penicillin/Streptomycin and L-glutamin were obtained from Biochrom (Berlin, Germany). Poly-D-lysine hydrobromide, Triton X100, Bovine Serum Albumin (BSA), 4′,6-Diamidine-2′-phenylindole dihydrochloride (DAPI), glycerol, 3-(4,5-dimethylthiazol-2-yl)-2,5-diphenyl tetrazolium bromide (MTT) and sucrose were obtained from Sigma-Aldrich Co. (St-Louis, USA). Dimethylsulfoxide (DMSO), trypan blue, paraformaldehyde, toluene, methanol, 2-isopropanol, acetonitrile, tris(hydroxymethyl)aminomethane (Tris) and ethylene glycol-bis(β-aminoethyl ether)-N,N,N',N'-tetraacetic acid (EGTA) from Carl Roth GmbH + Co. KG (Karlsruhe, Germany) were used. 3-(*N*-morpholino)propanesulphonic acid (MOPS) was purchased from ICN Biomedicals Inc. (Ohio, USA).

2.2. C_{60} fullerene synthesis

The pristine C_{60} fullerene aqueous colloid solution was prepared as described in [28] by C_{60} fullerene transfer from toluene to water using continuous ultrasound sonication. Obtained C_{60} colloid solution was characterized by high C_{60} fullerene concentration (2×10^{-4} M, purity 99%), stability and homogeneity.

2.3. Spectrophotometric analysis

Samples (100 µl of C_{60} colloid solution) were placed into a 96-well plate Sarstedt (Nümbrecht, Germany), C_{60} absorbance spectrum was measured with the multimode microplate spectrometer Tecan infinite M200 PRO (Grödig, Austria) at the following parameters: wavelength range 200–900 nm, wavelength step size: 2 nm, number of flashes per well: 10.

2.4. Cell culture

The human cancer cell line of leucosis origin – CCRF-CEM (ACC 240) – was purchased from the Leibniz Institute DSMZ-German Collection of Microorganisms and Cell Cultures. Cells were maintained in RPMI 1640 medium supplemented with 10% Fetal Bovine Serum, 1% Penicillin/Streptomycin and 2 mM Glutamine, using 25 cm^2 flasks at a 37 °C with 5% CO_2 in a humidified incubator Binder (Tuttlingen, Germany). The number of viable cells was counted using 0.1% trypan blue staining and a Roche Cedex XS Analyzer (Basel, Switzerland).

2.5. Immunofluorescence staining

CCRF-CEM cells (2×10^5/ml) were seeded in 6-well plates (Sarstedt, Nümbrecht, Germany) on cover slips (Carl Roth, Karlsruhe, Germany), previously coated with poly-D-Lysine, and incubated for 24 h. Cells were treated with 20 µM C_{60} colloid solution for further 24 h. Then cells were washed with PBS, stained with MitoTracker Orange FM (Invitrogen Molecular Probes, Carlsbad, USA) for 30 min at 37 °C and then fixed with 4% paraformaldehyde for 15 min at room temperature (RT) in the dark. After washing with PBS, cells were permeabilized with

0.2% Triton X100 for 10 min at RT and washed again with PBS. Blocking was performed using 10% BSA for 20 min with following washing in PBS. The primary monoclonal antibody IgG (developed in mouse) against C_{60} fullerene conjugated to thyroglobulin of bovine origin (dilution ratio of 1:30 in PBS/1.5%BSA, 1–10F-A8 Santa Cruz Biotechnology Inc., Santa Cruz, CA, USA) was added to the CCRF-CEM cells and incubated overnight at 4 °C in a humidified chamber. Then CCRF-CEM cells were incubated for 3 h at RT with a FITC-labeled polyclonal antibody against mouse IgG developed in rabbit (dilution ratio of 1:200 in PBS/1.5%BSA, F7506 Sigma-Aldrich Co., St-Louis, USA). Slides were washed between each step in three shifts of PBS for 15 min each. The coverslips were rinsed with dH_2O, incubated with nucleus staining antifade solution (0.6 μM DAPI, 90 mM p-Phenylenediamine in glycerol/PBS) for 2 h in the dark and sealed with slides. CCRF-CEM cells were observed using a Fluorescence Microscope Keyence BZ-9000 BIOREVO (Osaka, Japan) equipped with blue (λ_{ex} 377 nm, λ_{em} 447 nm), green (λ_{ex} 472 nm, λ_{em} 520 nm) and red (λ_{ex} 543 nm, λ_{em} 593 nm) filters with the acquisition software Keyence BZ-II Viewer (Osaka, Japan). The merged images and single cell fluorescence intensity profiles were processed with the Keyence BZ-II Analyzer software (Osaka, Japan).

2.6. High performance liquid chromatography-electro spray ionization-mass spectrometry (HPLC-ESI-MS)

The liquid chromatography separation and mass spectrometric detection were achieved by employing the Nexera HPLC system coupled to the LCMS-8040 Tandem Quadrupole Mass Spectrometer, equipped with an ESI source (Shimadzu, Kyoto, Japan). Chromatographic separation was performed using the column Eclipse XDV-C8 150 mm × 4,6 mm, 5 μm (Agilent, Santa Clara, USA). Optimized HPLS-ESI-MS conditions described in [35]. For data processing the software LabSolutions LCMS (Shimadzu, Kyoto, Japan) was used.

2.7. C_{60} fullerene extraction

CCRF-CEM cells (2×10^5/ml) were seeded in 6-well plate Sarstedt (Nümbrecht, Germany). After 24 h cells were incubated for 0–48 h in the presence of 20 μM C_{60}, washed with PBS three times and transferred to the dH_20. The freeze-thawing cycle was repeated three times. The probes were dried at 80 °C under reduced pressure. Toluene/2-propanol (6:1, v/v) was added in the final volume 0.5 ml, the mixture was sonicated for 1 h and centrifuged (70 min, 20238*g*). The toluene layer was analyzed with HPLC-ESI-MS.

2.8. Isolation of mitochondria

CCRF-CEM cells were incubated for 24 h in the presence of 20 μM C_{60} and the mitochondria fraction was isolated accordingly to [36]. Briefly, cell suspension (5×10^6/4 ml) was centrifuged at 600*g* at 4 °C for 10 min, cells were resuspended in 3 ml of ice cold isolation buffer (IB: 0.01 M Tris-MOPS, 1 mM EGTA/Tris, 0.2 M sucrose, pH 7.4) and homogenized in the teflon-glass potter on ice. The homogenate was centrifuged at 600*g* at 4 °C for 10 min. The collected supernatant (S1) was centrifuged at 7000*g* at 4 °C for 10 min. The pellet (P2) was resuspended in 200 μl ice-cold IB and centrifuged at 7000*g* at 4 °C for 10 min. The mitochondrial fraction obtained in pellet (P3) was used for extraction of C_{60} fullerene as well as for measurements of protein concentration [37] and succinate-reductase activity as mitochondrial marker [38]. The data concerning mitochondrial purity test available in [35].

2.9. Photodynamic therapy in vitro and cell viability assay

For cell viability assay, 10^4 cells/well were cultured in 96-well cell culture plates (Sarstedt, Nümbrecht, Germany) at for 24 h and then incubated for 24 h with 20 μM C_{60} and washed with PBS. Light irradiation was applied at the following wavelengths: UV – 365 nm Nichia SMD LED UV NCSU275, 140.6 mW/cm^2 (LUMITRONIX LED-Technik GmbH, Hechingen, Germany); violet – 405 nm high power single chip LED VL400-EMITTER, 108.3 mW/cm^2; green – 515 nm high power single chip LED APG2C1–515, 50.9 mW/cm^2; red – 650 nm, ELD-650-523, 5.1 mW/cm^2 (Roithner Lasertechnik GmbH, Vienna, Austria); red – 632 nm helium-neon 30 mW laser, 90 mW/cm^2 (Melles Griot, New York, USA). The light fluence was used in the range of 1–8 J/cm^2 for UV, 5–20 J/cm^2 for violet and green light and 1–80 J/cm^2 for red light. PBS was replaced with fresh medium immediately after irradiation. Control cells were incubated without exposure to fullerene treatment or light irradiation. After 24 h incubation cell viability was determined with MTT reduction assay. 10 μl of MTT solution (5 mg/ml in PBS) was added to each well and cells were incubated for 2 h at 37 °C. The culture medium was then replaced with 100 μl of DMSO, diformazan formation was determined by measuring absorption at 570 nm with a microplate reader Tecan Infinite M200 Pro (Männedorf, Switzerland).

2.10. Intracellular ROS-generation

To determine ROS production 2,7-dichlorofluorescin diacetate (DCFH-DA) (Sigma-Aldrich Co., St-Louis, USA) was applied. A 5 mM stock solution of DCFH-DA was prepared in DMSO, stored at −20 °C and diluted with PBS immediately before use. 10^4 cells were incubated in RPMI with 20 μM C_{60} for 24 h, irradiated (10 J/cm^2 405 nm LED) as indicated above, and washed once with PBS at 1 h and 3 h of further incubation. 5 μM DCF-DA was added and the fluorescence (λ_{ex} 488 nm, λ_{em} 520 nm) was recorded every 5 min during 50 min with the microplate reader Tecan Infinite M200 Pro (Männedorf, Switzerland). After 60 min incubation fluorescent images of cells were obtained with the Fluorescence Microscope Keyence BZ-9000 BIOREVO (Germany), equipped with a green filter (λ_{ex} 472 nm, λ_{em} 520 nm).

2.11. Caspase 3/7 activity

The CCRF-CEM cells were seeded into 96-well plates (10^4 cells/well) and incubated for 24 h. The cells were treated with 20 μM C_{60} for 24 h and irradiated (405 nm, 10 J/cm^2) irradiation as described above. Activity of caspases 3/7 was determined during 6 h period after light exposure using the Promega Caspase-Glo® 3/7 Activity assay kit (Madison, USA) according to the manufacturer's instructions. Briefly, the plates were removed from the incubator and allowed to equilibrate to RT for 30 min. After treatment, an equal volume of Caspase-Glo 3/7 reagent was added followed by gentle mixing with a plate shaker at 300 rpm for 1 min. The plate was then incubated at RT for 2 h. The luminescence of each sample was measured with the microplate reader Tecan Infinite M200 Pro (Männedorf, Switzerland).

2.12. Flow cytometry analysis

CCRF-CEM cells were seeded onto 6-well plates at a cell density of 2×10^5 cells/well in 2 ml of culture medium, incubated for 24 h, than treated with 20 μM C_{60} for 24 h and irradiated with 405 nm LED as described above. At 6 and 24 h incubation period the cells were harvested. Apoptosis was detected by Annexin V-fluorescein isothiocyanate/propidium iodide (Annexin V-FITC/PI) apoptosis detection kit (eBioscience™, San Diego, USA) according to the manufacturer's instructions. Briefly, cells were harvested and washed with Binding buffer. After addition of FITC-conjugated Annexin V cells were incubated for 15 min at RT in dark. Cells were washed with Binding buffer and at 10 min after propidium iodide addition were analyzed with the flow cytometer BD FACSJazz™ (Singapore). A minimum of 20,000 cells per sample were acquired and analyzed with the BD FACS™ software (Singapore).

2.13. Statistical analysis

All experiments were carried out with a minimum of four replicates. Data analysis was performed with the use of the GraphPad Prism 7 (GraphPad Software Inc., USA). Paired Student's *t*-tests were performed. Differences values $p < 0.05$ were considered to be significant.

3. Results and discussion

3.1. C_{60} fullerene uptake by leukemic cells and its intracellular distribution

The first requirement for any photosensitizing agent is an extensive penetration into the cancer cells since otherwise ROS generation is not sufficient to induce cell death. Effective cellular uptake of pristine C_{60} fullerene was shown in vitro on different cell lines, including human keratinocytes HaCaT and human lung carcinoma cells A549 [39], human monocyte-derived macrophage cells [40], mouse macrophages RAW 264.7 [41], human mammary epithelial cells MCF10A and MDA MB 231 [42]. Though the intracellular accumulation of nanostructures was proved, still little is known about its subcellular localization, as well as its ability to relocate and to realize effects at the level of intracellular compartments in cells of different types.

3.2. Qualitative analysis

The intracellular uptake and distribution of C_{60} fullerene was studied by fluorescent immunostaining of human leukemic CCRF-CEM cells using a FITC-labeled antibody against C_{60}. DNA-binding dye DAPI was used as a cell nucleus marker and MitoTracker Orange as a mitochondrial marker. No significant unspecific green FITC-fluorescence was observed in the control cells incubated in the absence of C_{60} fullerene. On Fig. 2B the images of CCRF-CEM cells stained after 24 h incubation with C_{60} are presented. No changes in nucleus fluorescence as compared with controls were found, whereas green fluorescent punctuated dots surrounding the nucleus were detected (Fig. 2B). The data showed that C_{60} fullerene could diffuse through the cell plasma membrane and locate in the perinuclear region of leukemic cells. Next, we have evaluated whether C_{60} fullerene could localize in the mitochondria membranes. The data of fluorescent microscopy verified a partial co-localization of C_{60} antibodies and the mitochondrial marker. The intensity profiles of the three fluorescence channels (Fig. 2C) for individual cells (Fig. 2A, B arrows) revealed the overlap of the green C_{60} fullerene and the red mitochondria signals. These data support the evidence of C_{60} fullerene localization in mitochondria of human leukemic cells.

3.3. Quantitative analysis

To study the accumulation dynamics we have extracted C_{60} fullerene from the cell homogenate as well as from the mitochondrial fraction and carried out liquid chromatography mass-spectrometry analysis. This method together with electro-spray ionization was previously reported to be an effective tool for C_{60} fullerene quantification in water samples [43], zebrafish embryo [44] and human skin keratinocytes HaCaT [25]. The method [35] enabled the quantitative analysis of C_{60} fullerene accumulation in CCRF-CEM cells. According to the data presented on Fig. 2D the intracellular content of C_{60} fullerene reached its maximum of $< 250\ ng/10^6$cells after 24 h of incubation. A subsequent minor decrease of C_{60} fullerene content in leukemic cells extract at 48 h could be accounted by its partial efflux from the cancer cells.

HPLC-ESI-MS analysis of C_{60} fullerene content in the mitochondria fraction showed accumulation of the nanostructure at a level of $< 180\ ng/10^6$ cells at 24 h that amounted to 72% of its overall content in cell extract. This data demonstrate that C_{60} fullerene predominantly accumulates within mitochondria. This could be explained by a high electronegativity of C_{60} fullerene and a resulting affinity to the mitochondria-associated proton pool [22,45]. According to density functional theory simulations, C_{60} fullerene diffuses into the protonated mitochondrial intermembrane space, where it interacts with up to 6 protons, acquiring a positive charge [34]. This phenomenon is common for other negatively charged carbon nanoparticles such as single walled carbon nanotubes [46,47]. These were shown to be localized in mitochondria of different cells, too (ASTC-a-1, MCF 7, COS 7, EVC304 and RAW264.7) [48].

3.4. LED-assisted photodynamic therapy in vitro

Photosensitizing effects of C_{60} fullerene and its derivatives are induced by different visible light sources including broadband mercury-vapor [11,27,31], halogen [2,19,49,50], tungsten-xenon [51,52] and fluorescent [53] lamps as well as sharp band lasers [2,16,53]. A recent study [54] demonstrates C_{60} fullerene photoinduced cytotoxic effects against leukemic cells after irradiation with the white light-emitting diode lamp with the board emission spectrum (420–700 nm). LEDs as a light-source for PDT have been explored previously and were shown to be more cost-effective and serviceable as clinical lamps or lasers [32–34]. The fractionation of light is a promising tool for the optimization of PDT in order to select the most effective combination of the photosensitizing agent and the light conditions such as light wavelength and fluence [1,51], that can be realized with the use of sharp spectrum LEDs. In this study we tested four high output light-emitting diode chips with 365, 405, 515 and 650 nm light irradiation.

The efficiency of light-induced excitation of photosensitizing agents substantially depends on their relative optical absorption extinction coefficients. The UV/Vis absorption spectrum (200–900 nm) of pristine C_{60} fullerene aqueous colloidal solution (Fig. 3A) has three intense absorption bands typical for C_{60} [28] with maxima at 220, 265, and 350 nm and a long broad tail up to the red region of the visible light. Fig. 3A demonstrates that the absorption spectrum of C_{60} fullerene and the spectra of the used LEDs are overlapping, suggesting that they could be applied for C_{60} photoexcitation.

After 24 h treatment with C_{60} fullerene leukemic cells were irradiated and at 48 h the cell viability was estimated with the MTT assay. As shown in Fig. 3B-D, the effect of light irradiation itself on CCRF-CEM cell viability depends on light wavelength. Irradiation of cells in the ultraviolet light at 365 nm was followed by decrease of cell viability. The effect became stronger with the increase of the light fluence. After irradiation with 8 J/cm^2 the viability was only 32% compared to viability of control cells in the dark. So the high toxic effects of UV light itself makes its application unfavorable. Irradiation with visible light was followed by less cytotoxic effect in comparison with UV irradiation even considering the fact, that the visible light was used at higher fluences. After irradiation with violet light at 405 nm at a maximal dose (20 J/cm^2) cell viability was decreased on 16% of the control level (Fig. 3C). Light irradiation at 405 nm is used in practice for the sterilization of both clinical and nonclinical environment due to the strong bactericidal activity [55,56], but its inactivating effect against mammalian cells is slight [55,57]. No significant toxic effect was observed after cells irradiation with green light at 515 nm and red light at 650 nm with fluence rate of 20 J/cm^2, the cell viability was 90% and 95% accordingly as compared with control (Fig. 3D and Fig. SI 1).

We next studied cell viability after treatment with C_{60} fullerene and photoexcitation of accumulated nanostructures. No cytotoxic effect was detected when CCRF-CEM cells were treated with C_{60} and kept in the dark. When cells were incubated for 24 h in the presence of 20 μM C_{60} fullerene and then irradiated with 365 nm or 405 nm LEDs, a substantial decrease of cell viability was observed at 24 h after light exposure (Fig. 3B and C). Combined treatment with C_{60} fullerene and UV 365 nm light at the doses of 2 and 4 J/cm^2 decreased cell viability up to 39% and 7% respectively as compared with control cells. The increase of UV LED light fluence up to 8 J/cm^2 was followed by almost total cell

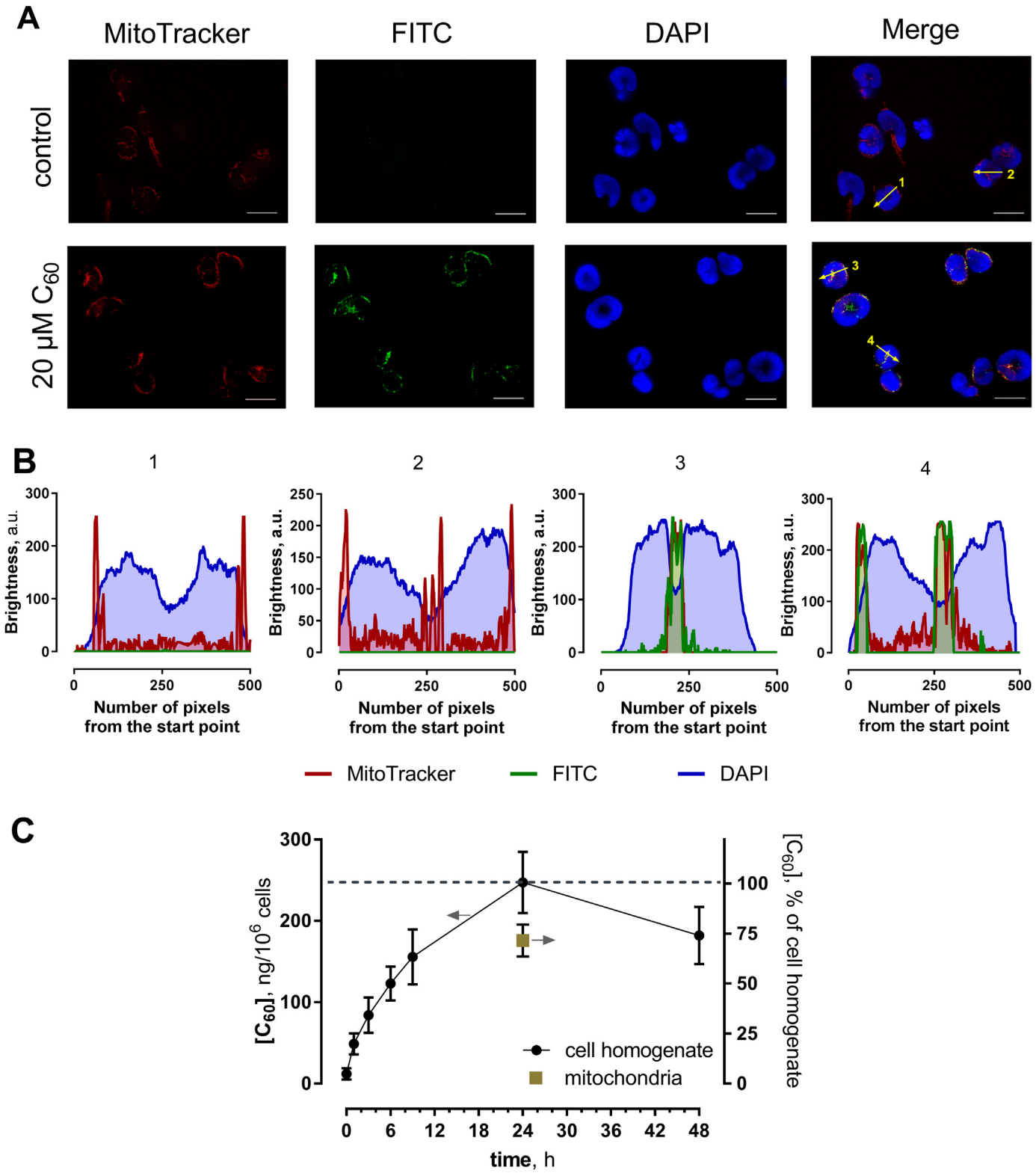

Fig. 2. Intracellular uptake and localization of C_{60} fullerene in CCRF-CEM cells. Fluorescence microscopy images of CCRF-CEM cells, stained with DAPI (blue), MitoTrecker (red) and FITC-labeled antibody against C_{60} fullerene (green): A – control cells, B – cells incubated for 24 h in the presence of 20 μM C_{60} fullerene, Scale bar 20 μm; C – Linear fluorescence profiles of single cell along the yellow arrows, indicated on the Merge images: 1, 2 – control cells, 3, 4 – cells incubated for 24 h in the presence of 20 μM C_{60}, D – HPLC-ESI-MS analysis of C_{60} fullerene content in cell extract and mitochondrial fraction after 0–48 h incubation of cells in presence of 20 μM C_{60} fullerene.

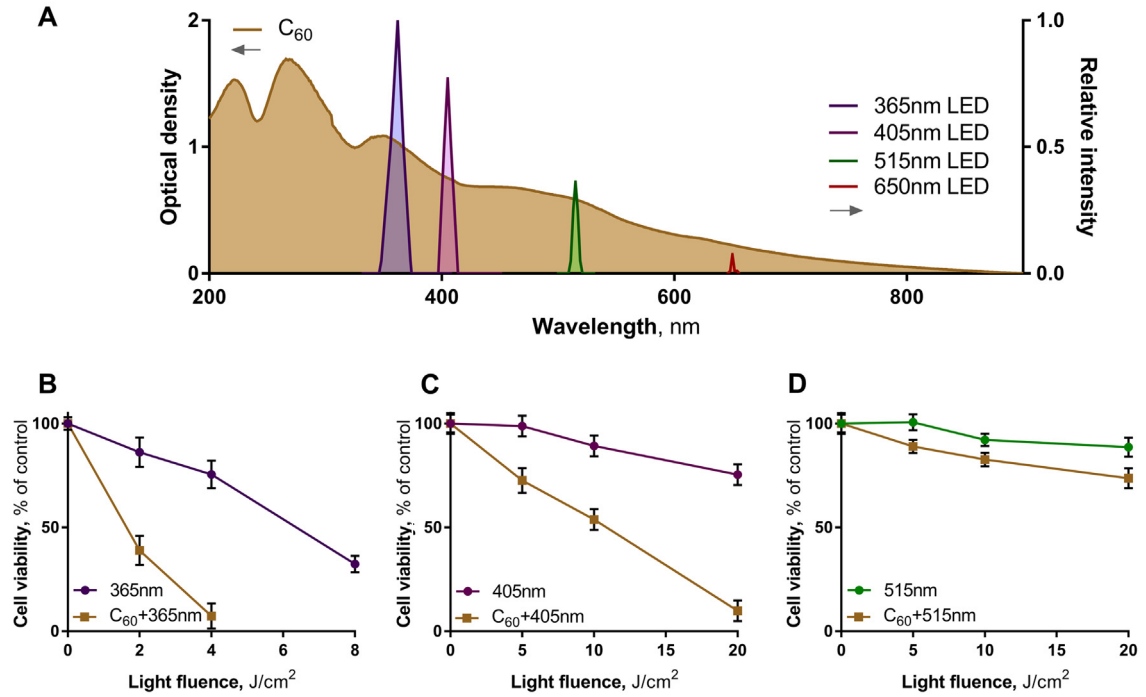

Fig. 3. In vitro C_{60} fullerene photodynamic therapy of human leukemic cells. A – Absorption spectrum of C_{60} fullerene and spectra of 365, 405, 515 and 650 nm LEDs; Viability of CCRF-CEM cells, incubated for 24 h in absence or presence of 20 μM C_{60} fullerene and irradiated with 365 (B), 405 (C) and 515 (D) nm LEDs at different light fluence.

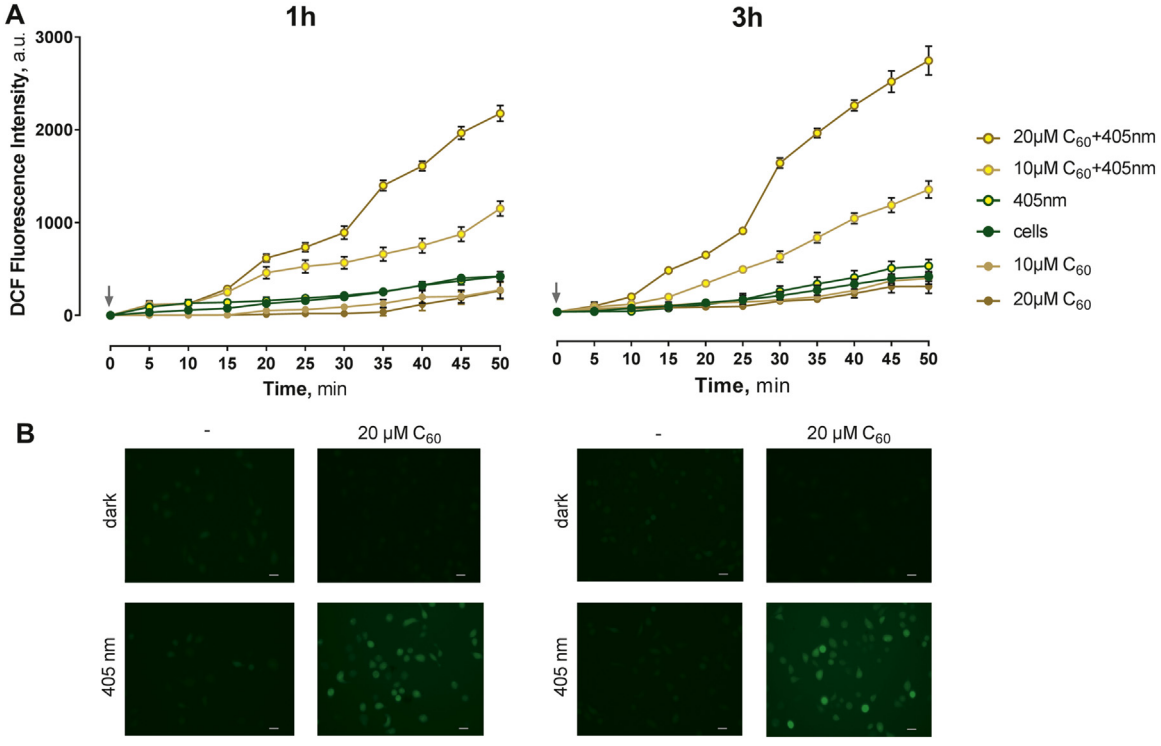

Fig. 4. Reactive oxygen species generation in CCRF-CEM cells (A) and fluorescent microscopy images (B) at 1 h and 3 h after treatment with either C_{60} fullerene or irradiation at 405 nm 10 J/cm^2 alone or their combination, Scale bar 20 μm.

death (Fig. 3B). Photoexcitation of accumulated C_{60} fullerene with violet 405 nm light at 5, 10 and 20 J/cm^2 light fluence caused cell viability decrease by 73%, 54% and 10%, respectively, as compared with control cells (Fig. 3C). C_{60} fullerene exhibited lower cytotoxicity under green 515 nm LED light irradiation. The viability of cells, treated with C_{60} fullerene for 24 h and exposed to the 5 and 10 J/cm^2 green LED light irradiation, was estimated to be around 85% with a further 10% decrease at 20 J/cm^2 (Fig. 3D). No fullerene cytotoxicity was observed at the further shift of the light wavelength into the red region of visible spectrum (Fig. SI 1). No significant effect on the viability of leukemic cells, incubated either in the presence or the absence of 20 μM C_{60} fullerene was detected under 650 nm LED light irradiation. Even

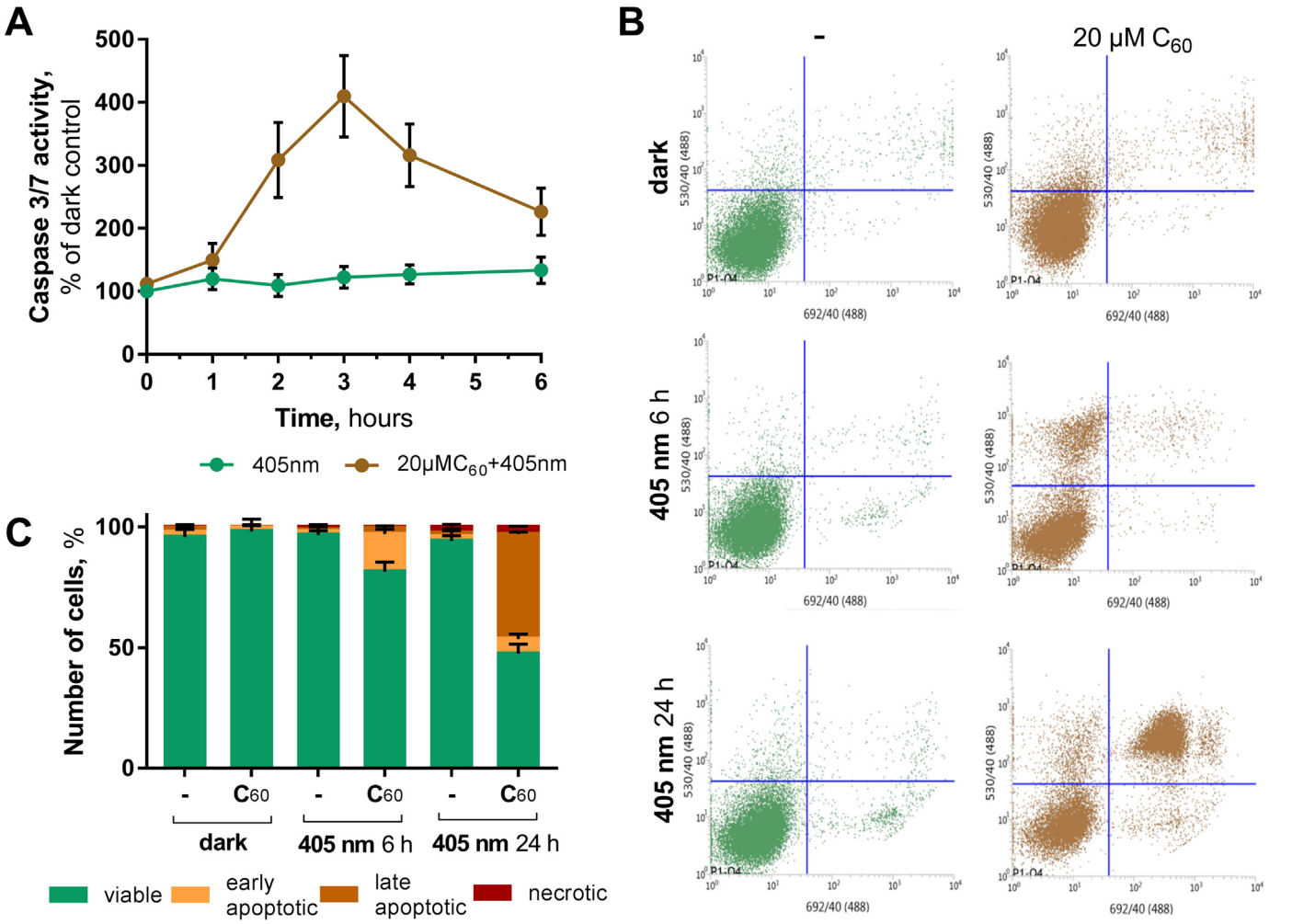

Fig. 5. Induction of apoptosis by C_{60} fullerene irradiation. A – Caspase 3/7 activity in CCRF-CEM cells, B – FACS histograms of CCRF-CEM cells, stained with Annexin V-FITC/PI (in each panel the lower left quadrant shows the content of viable, upper left quadrant – early apoptotic, upper right quadrant – late apoptotic, lower right quadrant – necrotic cells populations), C – Quantitative analysis of cell populations content, differentiated with double Annexin-FITC/PI staining after treatment of CCRF-CEM cells either with C_{60} fullerene alone or in combination with 405 nm light.

when we have applied intensities up to 80 J/cm^2 with the use of 650 nm helium-neon 30 mW laser no cytotoxic effect was observed because of low absorbance of longwavelength light by C_{60}. In order to increase the red light absorbance C_{60} fullerene can be modified with decacationic radicals [51] and additional red light harvesting chromophores [21,58] or excited with simultaneously delivered two near-infrared photons [2,59].

The anticancer effect of pristine C_{60} fullerene and LEDs light irradiation combination against human leukemic cells was shown to be strongly dependent on the light wavelength and fluence. The short-wavelength LEDs light irradiation was followed by most substantial decrease of leukemic cells viability, loaded with C_{60} fullerene. The efficiency of combined effect of C_{60} fullerene and LEDs light irradiation was proved to follow an expected order 365 nm > 405 nm > 515 nm > 650 nm (no effect). The obtained results indicate, that high output single chip 405 nm LED is the most favorable light source for C_{60} fullerene photodynamic therapy of human leukemic cells at intensities from 5 to 20 J/cm^2. The application of a 405 nm sharp spectrum high output LED chip for C_{60} fullerene photodynamic therapy allows to decrease the light dose in comparison with broad spectrum light sources, that are used at higher fluence rates of more than 100 J/cm^2 [2,26,50,60].

3.5. Reactive oxygen species generation

The efficient and continuous intracellular ROS production is a critical step for realization of a photoexcited C_{60} fullerene anticancer effect. ROS generation was estimated with the use of the fluorescence dye 2′,7′-dichlorodihydrofluorescein diacetate [61,62]. DCFH-DA is able to penetrate inside the cell, where it is deacyleted by esterases to its non-fluorescent form DCFH. Upon interaction with intracellular ROS DCFH is oxidized to DCF, which is characterized by a high green fluorescence. DCFH is mostly sensitive to hydroxyl radical, peroxonitrite and H_2O_2 [62]. CCRF-CEM cells, treated with 10 and 20 μM C_{60} fullerene were irradiated at 10 J/cm^2 405 nm. The ROS production was studied after 1 and 3 h of light exposure respectively. When DCFH-DA was added to untreated cells the slight continuous increase of fluorescence intensity was detected (Fig. 4A). Neither C_{60} fullerene nor light exposure alone caused significant changes in ROS generation in comparison with control, while at combined treatment with C_{60} fullerene and 405 nm LED light, ROS production in CCRF-CEM cells was shown to be increased dramatically. Irradiation of cells treated with 10 μM C_{60} was followed by 4-fold while treated with 20 μM C_{60} – by 8- and 10-fold increase of ROS level at 1 and 3 h respectively (Fig. 4A). The microscopy analysis of cells, presented on Fig. 4B, confirmed DCF fluorescent measurement data, thus, indicating that photoexcitation of accumulated C_{60} fullerene with 405 nm LED was followed by oxidative stress in

leukemic cells.

3.6. Apoptosis induction

The photosensitizing potential of intracellular accumulated C_{60} fullerene irradiated with 405 nm LED light was further studied by evaluation of the caspase 3/7 activity and plasma membrane phosphatidylserine translocation as primary markers of cell death by apoptosis. CCRF-CEM cells were incubated for 24 h in the presence or absence of C_{60} fullerene, irradiated with 405 nm LED and caspase 3/7 activity was measured during further 6 h incubation. We have shown that light irradiation alone had no effect on caspase 3/7 activity, while C_{60} fullerene photoexcitation was followed by 4-fold increase of caspase 3/7 activity at 3 h in comparison with control (Fig. 5A).

Exposure of phosphatidylserine on cell surface is proved to be an "eat me" signal, which facilitates phagocytic recognition of apoptotic cells and their destruction [63]. CCRF-CEM cells, treated with C_{60} and either kept in the dark or irradiated with 405 nm LED, were subjected to double staining with phosphatidylserine-binding Annexin V-FITC and DNA-binding dye propidium iodide. On FACS histograms (Fig. 5B) four populations of cells are presented according to green (annexin V-FITC) and red (PI) fluorescence intensities: viable (annexin V-FITC negative, PI negative), early apoptotic (annexin V-FITC positive, PI negative), late apoptotic (annexin V-FITC positive, PI positive) and necrotic (annexin V-FITC negative, PI positive) cells. Quantitative analysis of cell populations content at 6 and 24 h after combined treatment of CCRF-CEM cells with C_{60} and 405 nm light is presented on Fig. 5C. Neither treatment with 20 μM C_{60} nor 405 nm light irradiation alone had significant effect on cells distribution profiles, demonstrating a viability rate around 95%. Under combined action of C_{60} fullerene and 405 nm light a time-dependent increase in the content of apoptotic CCRF-CEM cells was detected, that reached level of 18% and 50% at 6 and 24 h after light exposure respectively, compared to 4% of control cells, treated with C_{60} fullerene and kept in the dark (Fig. 5B, C). The obtained data allow to conclude that toxic effect of C_{60} fullerene against CCRF-CEM cells after photoexcitation is realized by apoptosis induction.

4. Conclusions

With the use of immunocytochemical staining and mass spectrometry we have shown that pristine C_{60} fullerene was taken up by human leukemic CCRF-CEM cells from the media in a time-dependent manner, reaching a maximum intracellular level of almost 250 ng/10^6 cells at 24 h of incubation and was predominantly localized within mitochondria. The comparative analysis of a potential phototoxicity of C_{60} fullerene in human leukemic cells using LEDs of different wavelengths revealed that the most favorable effect was at 405 nm, 10 J/cm^2. No C_{60} fullerene neither 405 nm LED light alone impaired cell viability, while their combined action was followed by 46% cell viability decrease, 10-fold increase of reactive oxygen species generation, 4-fold increase of apoptosis-executive caspases 3/7 activity and plasma membrane phosphatidylserine externalization in 50% of cells. Our data suggest the use of C_{60} fullerene and 405 nm high power LED as a light source for photodynamic treatment of cancer cells.

Acknowledgments

We thank the German Academic Exchange Service (DAAD) for their support (scholarship for AG 57129429). TD acknowledges support by BMBF (Remis-3R, FKZ 031L0129B).

The authors are also very grateful to Karsten Lange (SLT Sensor- und Lasertechnik GmbH) for the measurements of LED light fluences and Dr. rer. nat. habil Catrin Wernicke for her support and informative discussions concerning immunocytochemical staining and caspases 3/7 assay.

Authors' contributions

The presented work was carried out in collaboration between all authors.

FM, TD, UR and OM coordinated the research work. SP and UR synthesized C_{60}. SG carried out the mass spectrometry. AG performed cell based assays and the statistical analysis. AG, OM and MF analyzed the data and wrote the manuscript. All authors discussed the results and commented on the manuscript.

Competing interests

The authors declare that they have no competing interests.

Appendix A. Supporting information

Supplementary data associated with this article can be found in the online version at http://dx.doi.org/10.1016/j.freeradbiomed.2018.06.022.

References

[1] D.E. Dolmans, D. Fukumura, R.K. Jain, Photodynamic therapy for cancer, Nat. Rev. Cancer 3 (2003) 380–387, http://dx.doi.org/10.1038/nrc1071.
[2] S.K. Sharma, L.Y. Chiang, M.R. Hamblin, Photodynamic therapy with fullerenes in vivo: reality or a dream? Nanomedicine 6 (10) (2011) 1813–1825, http://dx.doi.org/10.2217/nnm.11.144.
[3] J.N. Ribeiro, A.R. Silva, R.A. Jorge, Involvement of mitochondria in apoptosis of cancer cells induced by photodynamic therapy, J. Bras. Patol. Med. Lab. 40 (6) (2004) 383–390, http://dx.doi.org/10.1590/S1676-24442004000600005.
[4] P. Agostinis, K. Berg, K.A. Cengel, T.H. Foster, A.W. Girotti, S.O. Gollnick, S.M. Hahn, M.R. Hamblin, A. Juzeniene, D. Kessel, M. Korbelik, J. Moan, P. Mroz, D. Nowis, J. Piette, B.C. Wilson, J. Golab, Photodynamic therapy of cancer: an update, Cancer J. Clin. 61 (2011) 250–281, http://dx.doi.org/10.3322/caac.20114.
[5] R. Saini, C.F. Poh, Photodynamic therapy: a review and its prospective role in the management of oral potentially malignant disorders, Oral. Dis. 19 (2013) 440–451, http://dx.doi.org/10.1111/odi.12003.
[6] P. Keahey, P. Ramalingam, K. Schmeler, R.R. Richards-Kortum, Differential structured illumination microendoscopy for in vivo imaging of molecular contrast agents, Proc. Natl. Acad. Sci. USA 113 (39) (2016) 10769–10773, http://dx.doi.org/10.1073/pnas.1613497113.
[7] B.A. Flusberg, E.D. Cocker, W. Piyawattanametha, J.C. Jung, E.L. Cheung, M.J. Schnitzer, Fiber-optic fluorescence imaging, Nat. Methods 2 (12) (2005) 941–950, http://dx.doi.org/10.1038/nmeth820.
[8] S. Yano, S. Hirohara, M. Obata, Y. Hagiya, S. Ogura, A. Ikeda, H. Kataoka, M. Tanaka, T. Joh, Current states and future views in photodynamic therapy, J. Photochem. Photobio. C: Photochem. 12 (2011) 46–67, http://dx.doi.org/10.1016/j.jphotochemrev.2011.06.001.
[9] L. XiaoHui, Z. Cheng, L.G. Laurent, C. ChunYing, "Smart" nanomaterials for cancer therapy, Cancer Nanotechnol. 53 (11) (2010) 2241–2249, http://dx.doi.org/10.1007/s11426-010-4122-9.
[10] H.W. Kroto, J.R. Heath, S.C. O'Brien, R.F. Curl, R.E.C. Smalley, C_{60}: buckminsterfullerene, Nature 318 (1985) 162–163, http://dx.doi.org/10.1038/318162a0.
[11] P. Scharff, U. Ritter, O.P. Matyshevska, S.V. Prylutska, I.I. Grynyuk, A.A. Golub, Y.I. Prylutskyy, A.P. Burlaka, Therapeutic reactive oxygen generation, Tumori 94 (2008) 278–283 (PMID:18564617).
[12] A. Montellano, T. Ros, A. Bianco, M. Prato, Fullerene C_{60} as a multifunctional system for drug and gene delivery, Nanoscale 3 (2011) 4035–4041, http://dx.doi.org/10.1039/C1NR10783F.
[13] A.W. Jensen, S.R. Wilson, D.I. Schuster, Biological aspects of fullerenes, in: K. Kadish, R. Ruoff (Eds.), Fullerenes: Chemistry, Physics and Technology, John Wiley & Sons, 2000, pp. 437–465 . (https://10.1016/0968-0896)(96)(00081-8).
[14] G.D. Nielsen, M. Roursgaard, K.A. Jensen, S.S. Poulsen, S.T. Larsen, In vivo biology and toxicology of fullerenes and their derivatives, Basic Clin. Toxicol. 103 (2008) 197–208, http://dx.doi.org/10.1111/j.1742-7843.2008.00266.x.
[15] M.B. Spesia, M.E. Milanesio, E.N. Durantini, Fullerene derivatives in photodynamic inactivation of microorganisms, in: A. Ficai, A. Grumezescu (Eds.), Nanostructures for Antimicrobial Therapy, Elsevier, 2017, pp. 413–433, , http://dx.doi.org/10.1039/9781849733083-00161.
[16] M.A. Orlova, T.P. Trofimova, O.P. Orlov, O.A. Shatalov, Perspectives of fullerene derivatives in PDT and radiotherapy of cancers, Br. J. Med. Med. Res. 3 (4) (2013) 1731–1756, http://dx.doi.org/10.9734/BJMMR/2013/3453.
[17] A.P. Castano, T.N. Demidova, M.R. Hamblin, Mechanisms in photodynamic therapy: part one - photosensitizers, photochemistry and cellular localization, Photo. Photodyn. Ther. 1 (4) (2004) 279–293, http://dx.doi.org/10.1016/S1572-1000(05)00007-4.
[18] Ž. Lukšienė, Photodynamic therapy: mechanism of action and ways to improve the efficiency of treatment, Medicina 39 (12) (2003) 1137–1150 (PMID:14704501).
[19] Y. Yamakoshi, N. Umezawa, A. Ryu, K. Arakane, N. Miyata, Y. Goda, T. Masumizu,

T. Nagano, Active oxygen species generated from photoexcited fullerene (C_{60}) as potential medicines: O^{-}_{2} versus $^{1}O_{2}$, J. Am. Chem. Soc. 125 (2003) 12803–12809, http://dx.doi.org/10.1021/ja0355574.
[20] E. Otake, S. Sakuma, K. Torii, A. Maeda, H. Ohi, S. Yano, A. Morita, Effect and mechanism of a new photodynamic therapy with glycoconjugated fullerene, Photochem. Photobiol. 86 (2010) 1356–1363, http://dx.doi.org/10.1111/j.1751-1097.2010.00790.x.
[21] Z. Li, L.L. Pan, F.L. Zhang, X.L. Zhu, Y. Liu, Z.Z. Zhang, 5-Aminolevulinic acid-loaded fullerene nanoparticles for in vitro and in vivo photodynamic therapy, Photochem. Photobiol. 90 (2014) 1144–1149, http://dx.doi.org/10.1111/php.12299.
[22] S.M. Santos, A.M. Dinis, F. Peixoto, L. Ferreira, A.S. Jurado, R.A. Videira, Interaction of fullerene nanoparticles with biomembranes: from the partition in lipid membranes to effects on mitochondrial bioenergetics, Toxicol. Sci. 138 (1) (2014) 117–129, http://dx.doi.org/10.1093/toxsci/kft327.
[23] T.A. Stueckle, L. Sargent, Y. Rojanasakul, L. Wang, Genotoxicity and carcinogenic potential of carbon nanomaterials, in: C. Chen, H. Wang (Eds.), Biomedical Applications and Toxicology of Carbon Nanomaterials, John Wiley & Sons, 2016, pp. 267–332, , http://dx.doi.org/10.1002/9783527692866.ch10.
[24] R. Qiao, A.P. Roberts, A.S. Mount, S.J. Klaine, P.C. Ke, Translocation of C_{60} and its derivatives across a lipid bilayer, Nano Lett. 7 (3) (2007) 614–619, http://dx.doi.org/10.1021/nl062515f.
[25] S. Kato, R. Kikuchi, H. Aoshima, Y. Saitoh, N. Miwa, Defensive effects of fullerene-C_{60}/liposome complex against UVA-induced intracellular reactive oxygen species generation and cell death in human skin keratinocytes HaCaT, associated with intracellular uptake and extracellular excretion of fullerene-C_{60}, J. Photochem. Photobiol. B: Biol. 98 (2010) 144–151, http://dx.doi.org/10.1016/j.jphotobiol.2009.11.015.
[26] M. Akiyama, A. Ikeda, T. Shintani, Y. Doi, J. Kikuchi, T. Ogawa, K. Yogo, T. Takeya, N. Yamamoto, Solubilisation of [60] fullerenes using and evaluation of their photodynamic activities, Org. Biomol. Chem. 6 (2008) 1015–1019, http://dx.doi.org/10.1039/b719671g.
[27] A.P. Burlaka, Y.P. Sidorik, S.V. Prylutska, O.P. Matyshevska, O.A. Golub, Y.I. Prylutskyy, P. Scharff, Catalytic system of the reactive oxygen species on the C_{60} fullerene basis, Exp. Oncol. 26 (4) (2004) 326–327 (PMID:15627068).
[28] U. Ritter, Y.I. Prylutskyy, M.P. Evstigneev, N.A. Davidenko, V.V. Cherepanov, A.I. Senenko, O.A. Marchenko, A.G. Naumovets, Structural features of highly stable reproducible C_{60} Fullerene aqueous colloid solution probed by various techniques, Fuller. Nanotub. Carbon Nanostruct. 23 (2015) 530–534, http://dx.doi.org/10.1080/1536383X.2013.870900.
[29] S.V. Prylutska, O.P. Matyshevska, A.A. Golub, Y.I. Prylutskyy, G.P. Potebnya, U. Ritter, P. Scharff, Study of C_{60} fullerenes and C_{60}-containing composites cytotoxicity in vitro, Mater. Sci. Eng. 27 (2007) 1121–1124, http://dx.doi.org/10.1016/j.msec. 2006.07.009.
[30] S.V. Prylutska, I.I. Grynyuk, S.M. Grebinyk, O.P. Matyshevska, Y.I. Prylutskyy, U. Ritter, C. Siegmund, P. Scharff, Comparative study of biological action of fullerenes C_{60} and carbon nanotubes in thymus cells, Mat.-Wiss. Werkst. 40 (2009) 238–241, http://dx.doi.org/10.1002/mawe.200900433.
[31] S.V. Prylutska, I.I. Grynyuk, K.O. Palyvoda, O.P. Matyshevska, Photoinduced cytotoxic effect of fullerenes C_{60} on transformed T-lymphocytes, Exp. Oncol. 32 (1) (2010) 29–32 (PMID:20332760).
[32] C.-H. Yu, H.P. Lin, H.M. Chen, H. Yang, Y.P. Wang, C.P. Chiang, Comparison of clinical outcomes of oral erythroleukoplakia treated with photodynamic therapy using either light-emitting diode or laser light, Lasers Surg. Med. 41 (2009) 628–633, http://dx.doi.org/10.1002/lsm.20841.
[33] A. Erkiert-Polguj, A. Halbina, I. Polak-Pacholczyk, H. Rotsztejn, Light emitting diodes in photodynamic therapy in non-melanoma skin cancers – own observations and literature review, J. Cosmet. Laser Ther. 18 (2) (2016) 105–110, http://dx.doi.org/10.3109/14764172.2015.1114635.
[34] J. Hempstead, D.P. Jones, A. Ziouche, G.M. Cramer, I. Rizvi, S. Arnason, T. Hasan, J.P. Celli, Low-cost photodynamic therapy devices for global health settings: characterization of batterypowered LED performance and smartphone imaging in 3D tumor models, Sci. Rep. 5 (2015) 10093, http://dx.doi.org/10.1038/srep10093.
[35] A. Grebinyk, S. Grebinyk, S. Prylutska, U. Ritter, O. Matyshevska, T. Dandekar, M. Frohme. HPLC-ESI-MS Method for Fullerne C_{60} Mitochondrial Content Quantification. Data in Brief (Submitted for publication), 2018.
[36] C. Frezza, S. Cipolat, L. Scorrano, Organelle isolation: functional mitochondria from mouse liver, muscle and cultured filroblasts, Nat. Protoc. 2 (2) (2007) 287–295, http://dx.doi.org/10.1038/nprot.2006.478.
[37] M.M. Bradford, A rapid and sensitive method for the quantitation of microgram quantities of protein utilizing the principle of protein-dye binding, Anal. Biochem. 72 (1976) 248–254, http://dx.doi.org/10.1016/0003-2697(76)90527-3.
[38] R.J. Pennington, Mitochondrial succinate-tetrazolium reductase and adenosine triphosphatase, J. Biochem. 80 (1961) 649–654 (PMCID:PMC1243280).
[39] M. Horie, K. Nishio, H. Kato, N. Shinohara, A. Nakamura, K. Fujita, S. Kinugasa, S. Endoh, K. Yamamoto, O. Yamamoto, E. Niki, Y. Yoshida, H. Iwahashi, In vitro evaluation of cellular responses induced by stable fullerene C_{60} medium dispersion, J. Biochem. 148 (3) (2010) 289–298, http://dx.doi.org/10.1093/jb/mvq068.
[40] A.E. Porter, M. Gass, K. Muller, J.N. Skepper, P. Midgley, M. Welland, Visualizing the uptake of C_{60} to the cytoplasm and nucleus of human monocyte-derived macrophage cells using energy-filtered transmission electron microscopy and electron tomography, Environ. Sci. Technol. 41 (8) (2007), http://dx.doi.org/10.1021/es062541f.
[41] K.A. Russ, P. Elvati, T.L. Parsonage, A. Dews, J.A. Jarvis, M. Ray, B. Schneider, P.J. Smith, P.T. Williamson, A. Violi, M.A. Philbert, C_{60} fullerene localization and membrane interactions in RAW 264.7 immortalized mouse macrophages, Nanoscale 7 (8) (2016) 4134–4144, http://dx.doi.org/10.1039/c5nr07003a.
[42] N. Levi, R.R. Hantgan, M.O. Lively, D.L. Carroll, G.L. Prasad, C_{60}-Fullerenes: detection of intracellular photoluminescence and lack of cytotoxic effects, . J. Nanobiotechnol. 4 (2006) 14, http://dx.doi.org/10.1186/1477-3155-4-14.
[43] A. Wezel, V. Morinière, E. Emke, T. Laak, A. Hogenboom, Quantifying summed fullerene nC_{60} and related transformation products in water using LC LTQ orbitrap MS and application to environmental samples, Environ. Int. 37 (6) (2011) 1063–1067, http://dx.doi.org/10.1016/j.envint.2011.03.020.
[44] C.W. Isaacson, C.Y. Usenko, R.L. Tanguay, J.A. Field, Quantification of fullerenes by lc/esi-ms and its application to in vivo toxicity assays, Anal. Chem. 79 (2007) 9091–9097, http://dx.doi.org/10.1021/ac0712289.
[45] V.A. Chistyakov, E.V. Prazdnova, A.V. Soldatov, Yu.O. Smirnova, I. Alperovich, Can C_{60} fullerene demonstrate properties of mitochondria-targeted antioxidant from the computational point of view? Int. J. Biol. Biomed. Eng. 8 (2014) 59–62 ⟨https://www.naun.org/cms.action?id=7620⟩.
[46] F. Zhou, S. Wu, Y. Yuan, W.R. Chen, D. Xing, Mitochondria-targeting photoacoustic therapy using single-walled carbon nanotubes, Small 8 (10) (2012) 1543–1550, http://dx.doi.org/10.1002/smll.201101892.
[47] F. Zhou, S. Wu, B. Wu, W.R. Chen, D. Xing, Mitochondria-targeting single-walled carbon nanotubes for cancer photothermal therapy, Small 7 (19) (2011) 2727–2735, http://dx.doi.org/10.1002/smll.201100669.
[48] F. Zhou, D. Xing, B. Wu, S. Wu, Z. Ou, W.R. Chen, New insights of transmembranal mechanism and subcellular localization of noncovalently modified single-walled carbon nanotubes, Nano Lett. 10 (2010) 1677–1681, http://dx.doi.org/10.1021/nl100004m.
[49] F. Liao, Y. Saitoh, N. Miwa, Anticancer effects of fullerene [C_{60}] included in polyethylene glycol combined with visible light irradiation through ROS generation and DNA fragmentation on fibrosarcoma cells with scarce cytotoxicity to normal fibroblasts, Oncol. Res. 19 (2011) 203–216, http://dx.doi.org/10.3727/096504011X12970940207805.
[50] Y. Tabata, Y. Murakami, Y. Ikada, Photodynamic effect of polyethylene glycol-modified fullerene on tumor, Jpn. J. Cancer Res. 88 (1997) 1108–1116, http://dx.doi.org/10.1111/j.1349-7006.1997.tb00336.x.
[51] F.F. Sperandio, S.K. Sharma, M. Wang, S. Jeon, Y.-Y. Huang, T. Dai, S. Nayka, S.C.O.M. Sousa, L.Y. Chiang, M.R. Hamblin, Photoinduced electron-transfer mechanisms for radical-enhanced photodynamic therapy mediated by water-soluble decacationic C_{70} and $C_{84}O_{2}$ fullerene derivatives, Nanomedicine 9 (4) (2013) 570–579, http://dx.doi.org/10.1016/j.nano.2012.09.005.
[52] P. Mroz, Y. Xia, D. Asanuma, A. Konopko, T. Zhiyentayev, Y.Y. Huang, S.K. Sharma, T. Dai, U.J. Khan, T. Wharton, M.R. Hamblin, Intraperitoneal photodynamic therapy mediated by a fullerene in a mouse model of abdominal dissemination of colon adenocarcinoma, Nanomedicine 7 (6) (2011) 965–974, http://dx.doi.org/10.1016/j.nano.2011.04.007.
[53] C. Yu, P. Avci, T. Canteenwala, L.Y. Chiang, B.J. Chen, M.R. Hamblin, Photodynamic therapy with hexa(sulfo-n -butyl)[60]fullerene against sarcoma in vitro and in vivo, . J. Nanosci. Nanotechnol. 16 (2016) 171–181, http://dx.doi.org/10.1166/jnn.2016.10652.
[54] D. Franskevych, K. Palyvoda, D. Petukhov, S. Prylutska, I. Grynyuk, C. Schuetze, L. Drobot, O. Matyshevska, U. Ritter, Fullerene C_{60} penetration into leukemic cells and its photoinduced cytotoxic effects, Nanoscale Res. Lett. 12 (2017) 40, http://dx.doi.org/10.1186/s11671-016-1819-5.
[55] P. Ramakrishnan, M. Maclean, S.J. MacGregor, J.G. Anderson, M.H. Grant, Cytotoxic responses to 405nm light exposure in mammalian and bacterial cells: involvement of reactive oxygen species, Toxicol. In Vitro 33 (2016) 54–62, http://dx.doi.org/10.1016/j.tiv.2016.02.011.
[56] K. McKenzie, M. Maclean, M.H. Grant, P. Ramakrishnan, S.J. MacGregor, J.G. Anderson, The effects of 405 nm light on bacterial membrane integrity determined by salt and bile tolerance assays, leakage of UV-absorbing material and SYTOX green labelling, Microbiology 162 (9) (2016) 1680–1688, http://dx.doi.org/10.1099/mic.0.000350.
[57] P. Ramakrishnan, M. Maclean, S.J. MacGregor, J.G. Anderson, M.H. Grant, Differential sensitivity of osteoblasts and bacterial pathogens to 405-nm light highlighting potential for decontamination applications in orthopedic surgery, J. Biomed. Opt. 19 (10) (2014) 105001, http://dx.doi.org/10.1117/1.JBO.19.10.105001.
[58] D.J. Lee, Y.S. Ahn, Y.S. Youn, E.S. Lee, Poly(ethylene glycol)-crosslinked fullerenes for high efficient phototherapy, Polym. Adv. Technol. 24 (2) (2013) 220–227, http://dx.doi.org/10.1002/pat.3074.
[59] Y. Shen, A.J. Shuhendler, J.-J. Xua, H.-Y. Chen, Two-photon excitation nanoparticles for photodynamic therapy, Chem. Soc. Rev. 45 (2016) 6725, http://dx.doi.org/10.1039/C6CS00442C.
[60] G. Jiang, G. Li, Preparation, characterization, and properties of fullerene-vinylpyrrolidone copolymers, Biotechnol. Prog. 28 (1) (2012) 215–222, http://dx.doi.org/10.1002/btpr.707.
[61] E. Eruslanov, S. Kusmartsev, Identification of ROS Using oxidized DCFDA and flow-cytometry, Methods Mol. Biol. 594 (2010) 57–72, http://dx.doi.org/10.1007/978-1-60761-411-1_4.
[62] O. Myhre, J.M. Andersen, H. Aarnes, F. Fonnum, Evaluation of the probes 2',7'-dichlorofluorescin diacetate, luminol, and lucigenin as indicators of reactive species formation, Biochem. Pharmacol. 65 (2003) 1575–1582, http://dx.doi.org/10.1016/S0006-2952(03)00083-2.
[63] L. Suzuki, D.P. Denning, E. Imanishi, H.R. Horvitz, S. Nagata, Xk-related protein 8 and ced-8 promote phosphatidylserine exposure in apoptotic cells, Science 341 (6144) (2013) 403–406, http://dx.doi.org/10.1126/science.1236758.